PHYSICAL REVIEW C **96**, 025204 (2017)

Antiproton-proton annihilation into light neutral meson pairs within an effective meson theory

Ying Wang
Institut de Physique Nucléaire, Université Paris-Saclay, 91405 Orsay, France

Yury M. Bystritskiy* and Azad I. Ahmadov†
Institute for Nuclear Research, 141980 Dubna, Russia

Egle Tomasi-Gustafsson‡
IRFU, CEA, Université Paris-Saclay, 91191 Gif-sur-Yvette, France

(Received 1 June 2017; published 14 August 2017)

Antiproton-proton annihilation into light neutral mesons in the few GeV energy domain is investigated in view of a global description of the existing data and predictions for future work at the Antiproton Annihilation at Darmstadt (PANDA) experiment at the Facility for Antiproton and Ion Research (FAIR). An effective meson model earlier developed, with mesonic and baryonic degrees of freedom in s, t, and u channels, is applied here to $\pi^0\pi^0$ production. Form factors with logarithmic s and $t(u)$ dependencies are applied. A fair agreement with the existing angular distributions is obtained. Applying SU(3) symmetry, it is straightforward to recover the angular distributions for $\pi^0\eta$ and $\eta\eta$ production in the same energy range. A good agreement is generally obtained with all existing data.

DOI: 10.1103/PhysRevC.96.025204

I. INTRODUCTION

In a previous paper [1] we proposed an effective Lagrangian model with meson and baryon exchanges in s, t, and u channels (s, t, and u are standard kinematical Mandelstam variables) to describe the exclusive annihilation reaction of antiproton-proton annihilation into charged pion and kaon pairs in the energy domain $2.25(1.5) \leqslant \sqrt{s}(p_L) \leqslant 5.47(15)$ GeV (GeV/c) where $\sqrt{s}(p_L)$ is the total energy (the beam momentum) in the laboratory frame. This is the domain relevant to the Antiproton Annihilation at Darmstadt (PANDA) experiment at the Facility for Antiproton and Ion Research (FAIR) [2]. Data in this energy range are scarce, poorly constraining the models. To validate our approach we considered also pion-proton elastic scattering data through crossing symmetry.

We focus here on $\bar{p}p$ annihilation into two neutral light mesons (for a review, see [3,4]). A large amount of data on light meson production is expected in the near future. In the PANDA energy range, exclusive charged and neutral pion pair productions in $\bar{p}p$ collisions bring information on the nonperturbative structure of the proton and on the hadronization mechanisms.

In the low-energy region, particularly studied at the Low Energy Antiproton Ring (LEAR) at CERN, the angular distributions show a series of oscillations, typically reproduced by Legendre polynomials, describing contributions of higher excitation L waves. Antinucleon-nucleon potentials have been developed, using G-parity transformation of the nucleon-nucleon potential and adding an absorptive part in form of an imaginary Woods-Saxon potential [5–7]. In a microscopic approach, this process is understood as proceeding from the $\bar{p}p$ annihilation into the vacuum, ${}^3P_0$ state with spin-parity $J^P = 0^+$, $I = 0$ followed by momentum transfer with another quark or antiquark, and the ${}^3S_1$ state with spin-parity $J^P = 1^-$, $I = 0$ (the quantum numbers of a gluon) [8]. At low energies baryon exchange potential models have been applied successfully also for polarization observables at low energies [9]; however, the formalism becomes too complicated when the total energy is larger than 1 GeV. Effective Lagrangian models apply to a wide domain of reactions and kinematics, due also to the fact that beyond the exchanged particles, one may have freedom to choose ingredients as constants and form factors. The comparison with a quark exchange model in Ref. [1] shows that the experimental angular distributions are not reproduced satisfactorily in the considered energy range.

Increasing the energy, the angular distributions lose progressively their oscillating behavior. Above $\sqrt{s} = 2$ GeV, two-body processes become mostly peripheral and the angular distributions are peaked forward or backward, corresponding to small values of t or u, respectively. The cross section for pions emitted at $\cos\theta = 0$ [θ is the emission angle in the center-of-mass system (CMS)] shows a scaling behavior as a power of s, near to s^{-8}. This is consistent with QCD quark counting rules [10,11] that reproduce the measured energy dependences of exclusive hadron-hadron and meson-hadron cross sections in scattering as well as in annihilation regions, over a large range of θ, provided that the effective QCD scale Λ^2 is assumed small ($\Lambda \leqslant 0.1$ GeV).

We extend here the model developed in Ref. [1] to $\bar{p}p$ annihilation into neutral meson pairs. As in Ref. [1], t and u exchanges of nucleon and Δ are considered. First-order Born diagrams are calculated and form factors are added. Rather than monopole, dipole, or exponential form factors, i.e., the functional forms that can be found in the literature,

*bystr@theor.jinr.ru
†Permanent address: Institute of Physics, Azerbaijan National Academy of Sciences, Baku, Azerbaijan; ahmadov@theor.jinr.ru.
‡Corrresponding author: egle.tomasi@cea.fr

we propose s and t dependent logarithmic form factors, after being convinced that the Regge regime is not yet applicable in the considered energy region. Compared to charged pion production, the necessary modifications are the symmetrization of the final state for identical mesons and the nature of the exchanged meson in the s channel. Since a ρ meson cannot decay in a neutral pion pair, the lighter mesons that can be exchanged are the scalar f_0 and f_2 mesons, with masses and widths as [12]

$$\begin{aligned} f_0(500)I^G(J^{PC}) &= 0^+(0^{++}),\\ m_{f_0} &= (400\text{–}550)\ \text{MeV},\\ \Gamma_{f_0} &= (400\text{–}700)\ \text{MeV},\\ f_0(980)I^G(J^{PC}) &= 0^+(0^{++}),\\ m_{f_0} &= (990 \pm 20)\ \text{MeV},\\ \Gamma_{f_0} &= (40\text{–}100)\ \text{MeV},\\ f_2(1270)I^G(J^{PC}) &= 0^+(2^{++}),\\ m_{f_2} &= (1275{,}5 \pm 0.8)\ \text{MeV},\\ \Gamma_{f_2} &= (186.7 \pm 2.5)\ \text{MeV}. \end{aligned} \tag{1}$$

Pion emission around $\cos\theta = 0$ is driven by s-channel exchange. We limit our considerations to s-channel f_0- and f_2-meson exchange. In the case of f_0 we take "an effective f_0" with mass $M = 600$ MeV and width $\Gamma = 700$ MeV. In principle, other higher mass resonances that decay into $\pi^0\pi^0$ may be considered. However, they are suppressed outside the resonance peak due to the Breit-Wigner representation of the corresponding amplitudes. An additional suppression of radial excitations of these mesons is expected because their spatial density is less compact, making less probable the formation of a pion pair. Exclusive pion pairs are formed with the largest probability when the two $q\bar{q}$ pairs emerge from the vacuum in a physical space-time region with small dimension. It has been suggested that a Flatté distribution is more convenient for a light neutral scalar, in particular for $f_0(980)$ near the $K\bar{K}$ threshold [13]. In the present case, the contribution of the scalar mesons is not very large and the use of different, reasonable functions would change the final parameters within their errors. As we look for a simple parametrization with minimal number of parameters, a Breit-Wigner function is taken to reproduce the light scalar mesons.

We compare our calculation to the data on neutral pion (and other neutral meson) production, published by the FermiLab E760 Collaboration in the energy range $2.911 \leqslant \sqrt{s} \leqslant 4.274$ GeV [14]. The primary aim of that work was to study heavy meson resonances that couple to $\bar{N}N$, as charmonium. Moreover the study of the s dependence in terms of power laws showed that an approximate scaling is reached, but with a lower exponent than predicted. The measured angular distributions are limited to a central angular range, $|\cos\theta| \leqslant 0.66$. At the lowest energies, the $\pi^0\pi^0$ angular distribution shows a bump at $|\cos\theta| = 0$, which gradually disappears from 2.9 to 3 GeV, and can be reproduced including higher L multipolarities, only. To our knowledge, at present, no calculation attempting to reproduce the whole set of data from Ref. [14] exists in the literature.

Our aim is to build a reliable and coherent model that reproduces the basic features of neutral meson production in the energy range that will be investigated by the future PANDA experiment at FAIR. With the help of SU(3) symmetry, we apply our model to other neutral channels $\eta\eta$ and $\pi^0\eta$, where data are present. The model should have minimal ingredients and analytical expressions convenient to be included in the PANDARoot Monte Carlo simulation program.

II. FORMALISM

A. Kinematics and cross section

We consider the annihilation reaction

$$\bar{p}(p_1) + p(p_2) \to \pi^0(k_1) + \pi^0(k_2) \tag{2}$$

in CMS. The notation of four-momenta is shown in the parentheses. The following notations are used: $q_t = -p_1 + k_1$, $q_t^2 = t$, $q_u = -p_1 + k_2$, $q_u^2 = u$, and $q_s = p_1 + p_2$, $q_s^2 = s$, $s + t + u = 2M_N^2 + 2m_\pi^2$, M_N (m_π) is the nucleon (pion) mass [for reactions (20) and (21) the corresponding mass should be substituted]. The useful scalar product between four-vectors are explicitly written as

$$\begin{aligned} 2p_1k_2 &= 2k_1p_2 = M_N^2 + m_\pi^2 - u,\\ 2p_1k_1 &= 2k_2p_2 = M_N^2 + m_\pi^2 - t,\\ 2p_1p_2 &= s - 2M_N^2,\\ 2k_1k_2 &= s - 2m_\pi^2,\\ p_1^2 &= p_2^2 = M_N^2 = E^2 - |\vec{p}|^2,\\ k_1^2 &= k_2^2 = m_\pi^2 = \varepsilon^2 - |\vec{k}|^2. \end{aligned} \tag{3}$$

In particular,the final particle mass-shell conditions fix the energies $E_{1,2}$, velocity $\beta_{1,2}$, and modulus of the momentum $\vec{k}$ of the final particles (where "1" refers to the detected particle, and "2" to the partner):

$$E_{1,2} = \frac{s + M_{1,2}^2 - M_{2,1}^2}{2\sqrt{s}}, \quad \beta_{1,2} = \frac{\lambda^{1/2}(s, M_{1,2}^2, M_{2,1}^2)}{s + M_{1,2}^2 - M_{2,1}^2},$$
$$|\vec{k}| = \frac{1}{2\sqrt{s}}\lambda^{1/2}(s, M_1^2, M_2^2), \tag{4}$$

where $\lambda(x,y,z)$ is the so-called triangle function:

$$\lambda(x,y,z) = x^2 + y^2 + z^2 - 2xy - 2xz - 2yz. \tag{5}$$

The general expression for the differential cross section in the CMS of reaction (2) is

$$\frac{d\sigma}{d\Omega} = \frac{1}{2^8\pi^2}\frac{1}{s}\frac{\beta_\pi}{\beta_p}\overline{|\mathcal{M}|^2}, \quad \frac{d\sigma}{d\cos\theta} = 2E^2\beta_p\beta_\pi\frac{d\sigma}{dt}, \tag{6}$$

where $\mathcal{M}$ is the amplitude of the process, β_p (β_π) is the velocity and E (ε) is the energy of the proton (pion) in CMS. The phase volume can be transformed as $d\Omega \to 2\pi\, d\cos\theta$ due to the azimuthal symmetry of binary reactions. The total cross section then reads as

$$\sigma = \int \frac{\overline{|\mathcal{M}|^2}}{64\pi^2 s}\frac{|\vec{p}|}{|\vec{k}|}d\Omega, \tag{7}$$

where $|\vec{p}|$ is the initial momentum and $|\vec{k}|$ the momentum of the final detected particle in CMS. In the case of identical particles one should integrate only on half of the phase volume. $\overline{|\mathcal{M}|^2}$ is the squared matrix element of the process averaged over the spins of the initial particles.

B. Reaction mechanism

The formulas written above are model independent, i.e., they hold for any reaction mechanism. To calculate $\mathcal{M}$, one needs to specify a model for the reaction. In this work we consider the process (2) within the formalism of effective meson Lagrangian. The following contributions to the cross section for reaction (2) are calculated as illustrated in Fig. 1:

(i) Baryon exchange: t-channel nucleon (neutron) and Δ^+ exchange, Fig. 1(a), and the corresponding u-channel, crossed-leg diagrams, Fig. 1(b).
(ii) s-channel f_0, f_2 exchange, Fig. 1(c).

After the calculation of the coupling constant and matrix elements, the total matrix element squared averaged over the spin states of the initial particles is obtained as the sum of the squared of the matrix element for the individual contributions and the interferences among them. Identical particles in the final channel ($\pi^0\pi^0$ or $\eta\eta$) require us to symmetrize the amplitudes. The matrix element squared, obtained from the coherent sum of the amplitudes, is

$$\overline{|\mathcal{M}|^2} = \frac{1}{\sqrt{2}}\overline{|\mathcal{M}_p(t)+\mathcal{M}_{\Delta^+}(t)+\mathcal{M}_f(s)+\mathcal{M}_p(u)+\mathcal{M}_{\Delta^+}(u)|^2}. \tag{8}$$

Explicitly,

$$\begin{aligned}|\mathcal{M}(\bar{p}p\to\pi^0\pi^0)|^2 = |\mathcal{M}_{f_0}(s)|^2 + |\mathcal{M}_{f_2}(s)|^2 = \big\{&|\mathcal{M}_p(t)|^2+|\mathcal{M}_\Delta(t)|^2+|\mathcal{M}_p(u)|^2+|\mathcal{M}_\Delta(u)|^2\\ &+2\mathrm{Re}[\mathcal{M}_p(t)^*\mathcal{M}_p(u)+\mathcal{M}_p(t)^*\mathcal{M}_\Delta(t)+\mathcal{M}_p(t)^*\mathcal{M}_\Delta(u)+\mathcal{M}_p(u)^*\mathcal{M}_\Delta(t)+\mathcal{M}_p(u)^*\mathcal{M}_\Delta(u)]\big\}\\ &+\sqrt{2}\mathrm{Re}[\mathcal{M}^*_{f_0}(s)\mathcal{M}_{f_2}(s)+\mathcal{M}_p(t)\mathcal{M}^*_{f_0}(s)+\mathcal{M}_p(u)\mathcal{M}^*_{f_0}(s)+\mathcal{M}_\Delta(t)\mathcal{M}^*_{f_0}(s)+\mathcal{M}_\Delta(u)\mathcal{M}^*_{f_0}(s)\\ &+\mathcal{M}^*_p(t)\mathcal{M}_{f_2}(s)+\mathcal{M}^*_p(u)\mathcal{M}_{f_2}(s)+\mathcal{M}^*_\Delta(t)\mathcal{M}_{f_2}(s)+\mathcal{M}^*_\Delta(u)\mathcal{M}_{f_2}(s)].\end{aligned} \tag{9}$$

Taking into account the phase space and the flux, the expression for the total cross section is

$$\frac{d\sigma}{d\Omega}(\bar{p}p\to\pi^0\pi^0) = \frac{1}{2^8\pi^2}\frac{1}{s}\frac{\beta_\pi}{\beta_p}|\mathcal{M}(\bar{p}p\to\pi^0\pi^0)|^2, \tag{10}$$

or

$$\frac{d\sigma}{d\cos\theta}(\bar{p}p\to\pi^0\pi^0) = \frac{1}{2^7\pi}\frac{1}{s}\frac{\beta_\pi}{\beta_p}|\mathcal{M}(\bar{p}p\to\pi^0\pi^0)|^2. \tag{11}$$

For the explicit expressions of the t- and u-channel N and Δ amplitudes, in Eq. (9) we refer to the Appendix of Ref. [1]. Coupling constants are fixed from the known decays of the particles when possible, otherwise values from the effective potentials as in [15] are used. Values for x and widths are taken from the PDG [12]. The relevant formulas for the amplitudes and their interferences are given in Appendixes A and B.

Let us consider $f_0(500)$ also called the σ meson, the lowest isoscalar scalar particle, with spin zero and positive parity, and the next higher L contributions, the $f_2(1270)$ with spin 2 and positive parity. Both decay dominantly into two neutral pions (see Fig. 2).

The $f_{0,2}$ propagators are taken as a Breit-Wigner function

$$\frac{1}{q_s^2 - m^2_{f_{0,2}} + i\sqrt{q_s^2}\,\Gamma_{f_{0,2}}(q_s^2)}, \tag{12}$$

and the transferred momentum is $q_s = p_1 + p_2 = k_1 + k_2$, $q_s^2 = s$.

The $f_0\pi\pi$ vertex is $-ig_{f_0\pi\pi}$, with $g_{f_0\pi\pi}$ the constant for the decay $f_0\to\pi^0\pi^0$ (see Appendix A). The final expression for the width is

$$\Gamma_{f_0} = \frac{1}{16 m_{f_0}\pi} g^2_{f_0\pi\pi}\sqrt{1-\frac{4m_\pi^2}{m_{f_0}^2}}, \tag{13}$$

where by taking the value $\Gamma_{f_0} = 700\pm150$ MeV (in the range suggested by PDG [12]), one finds $g_{f_0\pi\pi} = 4.08\pm1.3$ GeV.

The f_0NN vertex is $-ig_{f_0NN}$ where $g_{f_0NN} = 5$ GeV is the coupling constant from Ref. [15].

The expression for the width of the decay $f_2\to\pi\pi$ is (see Appendix B)

$$\Gamma_{f_2} = \frac{g^2_{f_2\pi\pi}}{16 m_{f_2}\pi}|\mathcal{M}(f_2\to\pi\pi)|^2\sqrt{1-\frac{4m_\pi^2}{m_{f_2}^2}}. \tag{14}$$

Taking the value $\Gamma_{f_2} = (0.1867\pm0.0025)$ GeV, one finds $g_{f_2\pi\pi} = (19\pm0.26)\ \mathrm{GeV}^{-1}$.

The vertex $f_2\to pp$ then is written as

$$(-i)g_{f_2pp}\gamma_\mu(p_1-p_2)_\nu\chi^{\mu\nu}, \tag{15}$$

where g_{f_2pp} is considered as a fitting parameter and $\chi^{\mu\nu}$ is defined in Appendix B.

III. RESULTS

The following procedure was applied in order to reproduce the collected data basis. The data on neutral pion angular distributions from Ref. [14] were first reproduced best, with

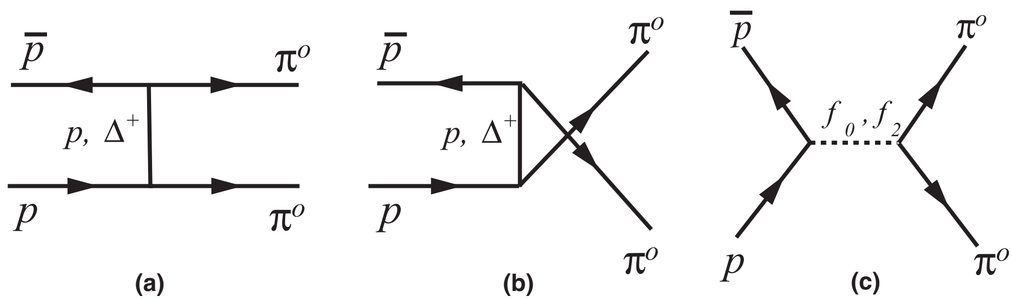

FIG. 1. Feynman diagrams for different exchanged particles for the reaction $\bar{p} + p \to \pi^0 + \pi^0$.

particular attention to the s dependence of the cross section. The necessary number of parameters is very limited and we checked that the results are quite stable toward a change of the parameters in a reasonable interval.

The composite nature of the hadrons should be taken into account in the calculation of the observables. To find the best description of the data in wide energy and angular ranges, different choices for form factors can be found in the literature: monopole, dipole, exponential, etc. In Ref. [1] a function of the logarithmic type turned out to reproduce best the measured angular and energy dependencies. The background of this choice is a QCD derivation from Refs. [16,17] that relates the asymptotic behavior of form factors to the quark contents of the participating hadrons. It is also known that a logarithmic dependence of the $\bar{p}p$ cross section reproduces quite well the background for resonant processes [18,19].

The logarithmic functional form is

$$F^L_{N,\Delta}(x) = \frac{\mathcal{N}_{N,\Delta}\ M_0^4}{\left[\left(x - \Lambda^2_{N,\Delta}\right) \ln \frac{(x-\Lambda^2_{N,\Delta})}{\Lambda^2_{\mathrm{QCD}}}\right]^2}, \quad x = s,t,u,$$
$$M_0 = 3.86 \ \mathrm{GeV}, \quad \Lambda_{\mathrm{QCD}} = 0.3 \ \mathrm{GeV}, \tag{16}$$

where M_0 is a scale parameter that has been inserted to conserve units, Λ_{QCD} is the QCD scale parameter. $\mathcal{N}_{N,(\Delta)} = 0.361 \pm 0.006(0.041 \pm 0.003)$ is a normalization constant. $\Lambda_{N,(\Delta)} = 2.25 \pm 0.09(1.05 \pm 0.04)$ GeV is a "slope" parameter which values were determined from a fit on the available data on charged pion production. A summary of parameters is listed in Table I for nucleon and Δ exchange.

For neutral pion pair production, the first attempt was to apply the same form factors and the same parameters as for the charged pion data for $t(u)$ N and Δ exchanges from [1], the s channel being calculated apart because physics requires the exchange of different mesons. Similar to charged meson production, first we apply the form factor $F^L_{N,\Delta}$ (Eq. 16) which depends on momentum transfer (t or u) to take into account the composite nature of the particle in the interaction point. Second, we use the factor $F^L_{N,\Delta}(s)$ which effectively takes into account pre-Regge regime excitations of higher resonances in the intermediate state. This leads to an effective form factor as the product:

$$\widetilde{F}_{N,\Delta}(s,t) = F^L_{N,\Delta}(s) F^L_{N,\Delta}(t)$$
$$\text{or} \quad \widetilde{F}_{N,\Delta}(s,u) = F^L_{N,\Delta}(s) F^L_{N,\Delta}(u), \tag{17}$$

containing the same set of parameters for the s and t (u) dependencies, but different for N and Δ exchanges. The fit does not require independent parameters for s and t (u) dependencies. The behavior of the total cross section for charged and neutral pion pair production is, however, very different. A possibility for recovering the $\pi^0\pi^0$ data is to modify the s-dependent part of the logarithmic form factors by adding an additional energy dependence to the parameters:

$$\mathcal{N}(s)_{p,\Delta} \to \mathcal{N}(s)_{p,\Delta} - e^{\frac{p^{\mathcal{N}}_{p,\Delta}(s)}{\sqrt{s}}},$$
$$\Lambda(s)^2_{p,\Delta} \to \Lambda(s)^2_{p,\Delta} - e^{\frac{p^{\Lambda}_{p,\Delta}(s)}{\sqrt{s}}}. \tag{18}$$

In Fig. 3 one can see the effect of the introduced s dependence. The parameters converge at high energies, whereas for $\sqrt{s} \leqslant 3.5$ GeV they deviate essentially, giving further reduction of the cross section. The s-independent parameters are fixed as in Table II.

The form factor for the f_0NN vertex is taken of monopole form:

$$\mathcal{F}_{f_0}(s) = \frac{F^2_{f_0}}{F^2_{f_0} + \left(m^2_{f_0} - s\right)}, \tag{19}$$

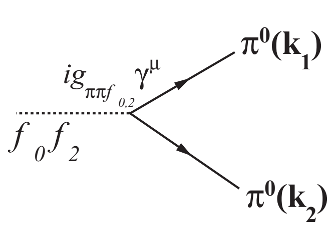

FIG. 2. f_0 and f_2 decay into a pion pair.

TABLE I. Parameters for the logarithmic form factors of Eq. (17).

Parameter	Value
$\mathcal{N}_N$	0.361 ± 0.006
$\mathcal{N}_\Delta$	0.041 ± 0.003
Λ^2_N	(2.25 ± 0.09) GeV^2
Λ^2_Δ	(1.05 ± 0.04) GeV^2

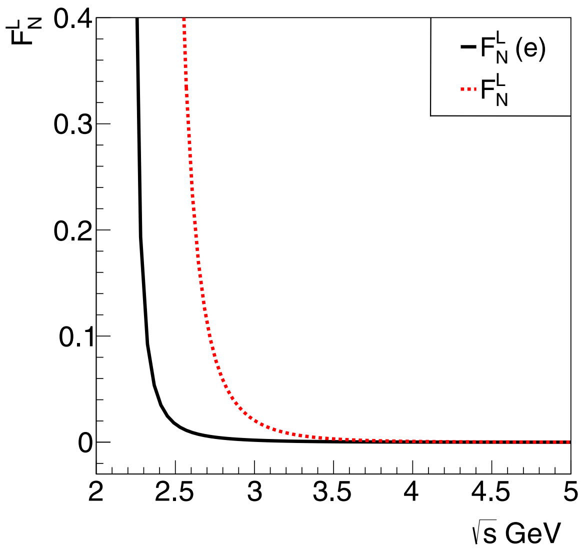

FIG. 3. Energy dependence of the logarithmic form factors without (red, dashed line) and with (black, solid line) exponential correction.

TABLE II. Parameters for the s-dependent term of the logarithmic form factors for $\bar{p}p \to \pi^0\pi^0$.

Parameter	Value (GeV)
$p_p^{\mathcal{N}}(s)$	-3.013 ± 0.210
$p_\Delta^{\mathcal{N}}(s)$	-5.959 ± 0.205
$p_p^{\Lambda}(s)$	4.047 ± 0.019
$p_\Delta^{\Lambda}(s)$	3.141 ± 0.002

with $F_{f_0} = 1.17 \pm 0.051$ GeV. In addition, similar to the charged pion calculation, the phase $\Phi_f = e^{i\pi\phi_f}$ is added for the exchanged meson in the s channel with ϕ_f equal to unity.

IV. COMPARISON WITH EXISTING DATA

The fitted plots and data from Ref. [14] are shown in Fig. 4, in the energy range $2.911 \leqslant \sqrt{s} \leqslant 3.686$ GeV. The data were measured in regular intervals, with a gap between 3.097 and 3.526 GeV which separates the data into a lower energy region ($2.911 \leqslant \sqrt{s} \leqslant 3.097$ GeV) and a higher energy region ($3.526 \leqslant \sqrt{s} \leqslant 3.686$ GeV). In the lower energy region, a bump produced by higher L resonances appears around

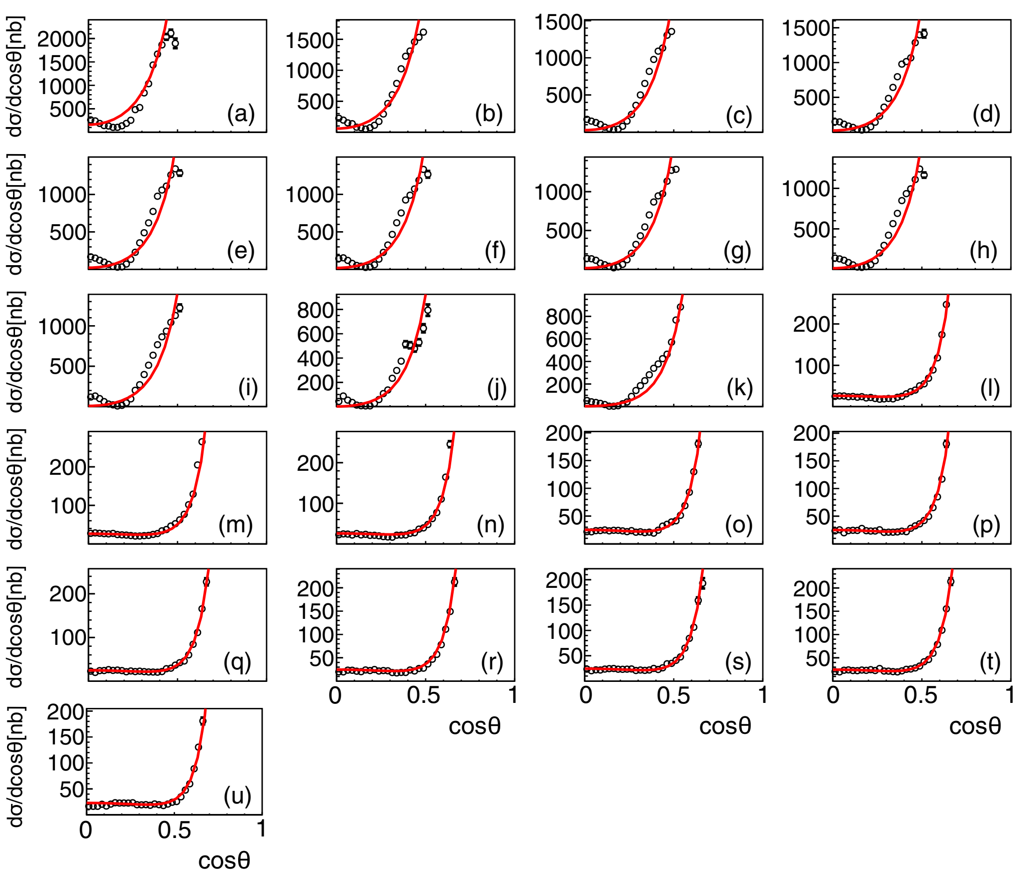

FIG. 4. Angular distribution for the reaction $\bar{p}p \to \pi^0\pi^0$ in CMS in the energy range $2.911 \leqslant \sqrt{s} \leqslant 3.686$ GeV. The data (open circles) are from Ref. [14]: $\sqrt{s} = 2.911$ GeV (a); 2.950 GeV (b); 2.975 GeV (c); 2.979 GeV (d); 2.981 GeV (e); 2.985 GeV (f); 2.990 GeV (g); 2.994 GeV (h); 3.005 GeV (i); 3.050 GeV (j); 3.097 GeV (k); 3.524 GeV (l); 3.526 GeV (m); 3.556 GeV (n); 3.591 GeV (o); 3.595 GeV (p); 3.613 GeV (q); 3.616 GeV (r); 3.619 GeV (s); 3.621 GeV (t), 3.586 GeV (u). The calculation is the solid, red line.

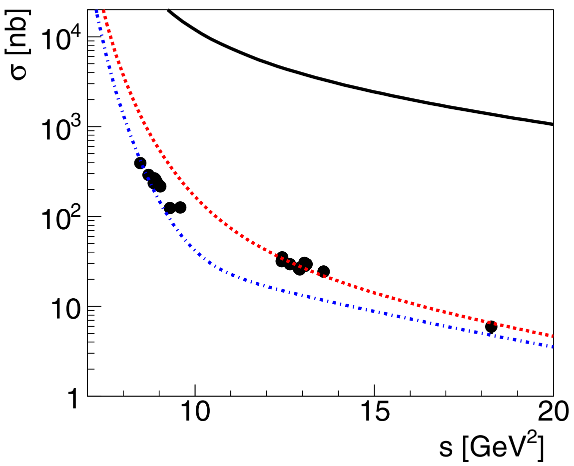

FIG. 5. Integrated cross section for the reaction $\bar{p}p \to \pi^0\pi^0$. The data are obtained by the integration of the partial differential cross section in the available range: $0 < \cos\theta < 0.48$ up to $\sqrt{s} = 3.2$ GeV, and $0 < \cos\theta < 0.66$ above $\sqrt{s} = 3.6$ GeV, Ref. [14]. The present calculation covering the range $0 < \cos\theta < 0.48$ (blue dash-dotted line) and $0 < \cos\theta < 0.66$ (red dashed line) is also shown. The integration in the whole angular range is shown as a black, solid line.

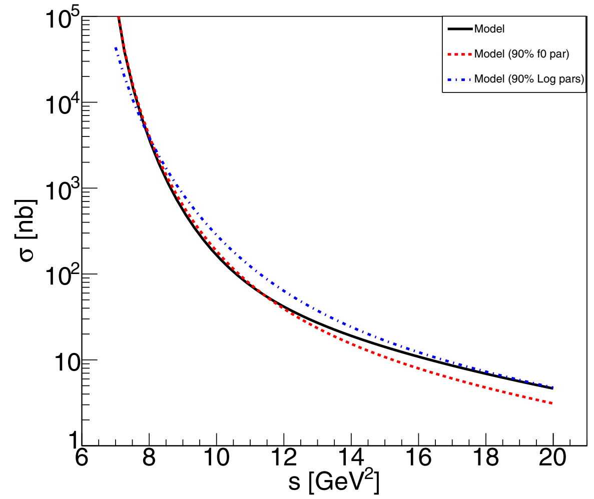

FIG. 6. Parameter dependence of the cross section for the reaction $\bar{p}p \to \pi^0\pi^0$, integrated for $|\cos\theta| \leqslant 0.66$. The calculation with the nominal parameter is shown (black solid line), together with the calculation corresponding to 10% decrease of the f_0 parameters (red dashed line) and to 10% decrease of the logarithmic form factor parameters (blue dash-dotted line).

$\cos\theta = 0$. It cannot be reproduced by the f_0 and f_2 mesons considered in the s channel, and it disappears at higher energies. We did not attempt to add higher resonances. More precise data are expected from PANDA in a larger angular range, better constraining the model.

Note that good agreement can be found when neglecting the f_2 contribution. The s dependence for the cross section of neutral pion production from 5 to 20 GeV^2 is shown in Fig. 5, where the experimental point is obtained integrating the data from Ref. [14] in the available angular range. The calculation is integrated in the same angular range $0 < \cos\theta < 0.66$ or 0.48. The calculation reproduces well the integrated data. Note that the available data cover a reduced angular distribution, whereas the very forward and backward regions give the largest contribution to the total cross section.

To appreciate the the sensitivity of the calculation to a selected choice of parameters, in Fig. 6 the cross section, integrated for $0 < \cos\theta < 0.66$, is reported (black solid line) together with the result of the calculation when decreasing by 10% the parameters of f_0 (red dashed line) and of the logarithmic form factor (blue dash-dotted line).

A. Higher energy set

The case of the set of data at $\sqrt{s} = 4.274$ GeV is peculiar. The data correspond to the higher energy available, and show a discontinuity with respect to the other sets. In particular the bump for $\cos\theta = 0$ evolves definitely into a dip. To reproduce this dip, the $L = 2$ f_2 meson is added. The form factor of f_2NN is taken as a monopole, Eq. (19), similar to f_0, and the relative phase is also taken as unity. Concerning the higher energy, the contribution from the f_0 meson is suppressed by the fitting procedure. The new parameters for the s channel are listed in the Table III, the other parameters are fixed as in Tables I and II.

The different components are visible in Fig. 7. One can see that the shape of the angular distribution is very well reproduced by the f_2 contribution. The Δ contribution overcomes the N term. The angular distribution is limited and one cannot draw firm conclusions on the t- and u-channel interplay of the different contributions. A very good agreement is obtained by fitting this set of data with the present model.

Applying SU(3) symmetry, one can connect other neutral channels. As we see in the next section, it works relatively well.

B. Reactions $\bar{p} + p \to \pi^0 + \eta$ and $\bar{p} + p \to \eta + \eta$

The two-body channels

$$\bar{p}(p_1) + p(p_2) \to \eta(k_1) + \eta(k_2), \tag{20}$$

$$\bar{p}(p_1) + p(p_2) \to \eta(k_1) + \pi^0(k_2) \tag{21}$$

involve mesons that are related by SU(3) symmetry, as π, η, and η' are members of a single nonet. Having a model that reproduces consistently angular distributions and cross sections for $\pi^0 + \pi^0$, based on s, t, and u channels, the

TABLE III. Parameters of form factors for f_0 and f_2 mesons at $\sqrt{s} = 4.274$ GeV.

Parameter	Value
F_{f_0}	0.870 ± 0.014 GeV
F_{f_2}	0.187 ± 0.001 GeV
χ^2/ndf	0.787

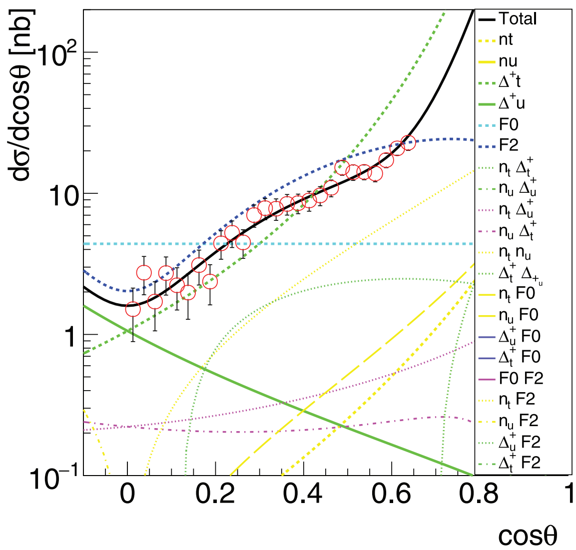

FIG. 7. Angular distribution for reaction $\bar{p}p \to \pi^0\pi^0$ at $\sqrt{s} = 4.274$ GeV [14] with the different components. The parameters are listed in Table III.

amplitudes for the decay to the channels of reactions (2), (20), and (21) are related by the SU(3) symmetry. Taking into account that, in principle, $\bar{p}p$ does not couple directly to $s\bar{s}$, the following relations hold:

$$
\begin{aligned}
f(\pi^0\eta) &= f(\pi^0+\pi^0)\cos\Theta,\\
f(\eta\eta) &= f(\pi^0+\pi^0)\cos^2\Theta, \qquad (22)
\end{aligned}
$$

where $\Theta \simeq 45^\circ$ is the pseudoscalar mixing angle [20].

The procedure follows the one derived above for $\pi^0\pi^0$. The masses have to be changed correspondingly in the calculation of the kinematics and amplitudes. Moreover, in the case of reaction (21) the fact that the final state is not symmetric induces a backward-forward asymmetry. Applying SU(3) symmetry and taking into account the kinematics difference due to the masses, the model is applied in the energy range $2.911 \leqslant \sqrt{s} \leqslant 3.617$ GeV. The results are shown in Figs. 8 and 9 for reactions (20) and (21), respectively. The agreement is very good without readjusting the parameters. The model is able to reproduce the data in the backward and forward regions. Similar to $\pi^0\pi^0$ it is expected that the bump around $\cos\theta = 0$ is not described, because it needs to include additional contributions. For the higher energy $\sqrt{s} = 4.274$ GeV, the data sets for $\eta\eta$ and $\eta\pi^0$ production have large error bars and a few points are measured. Precise data are expected from the PANDA experiment to fill this region.

V. CONCLUSIONS

A model built on the effective meson Lagrangian has been applied to two neutral pion production in proton-antiproton

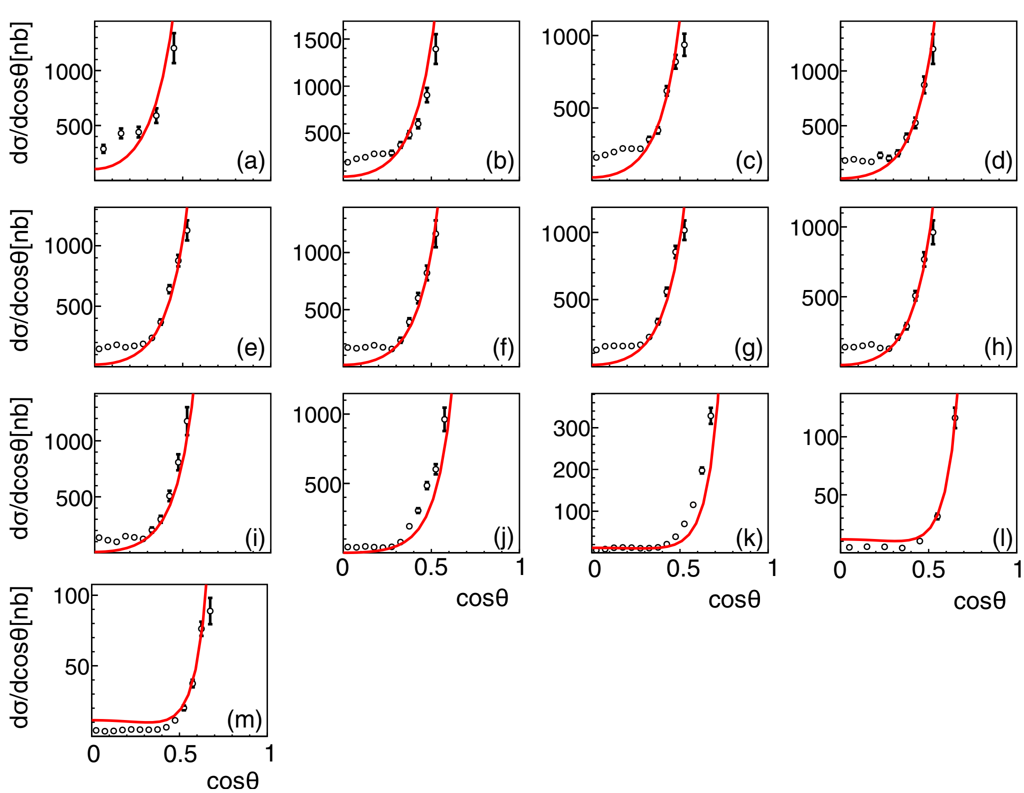

FIG. 8. Angular distribution for $\bar{p}p \to \eta\eta$ in CMS in the energy range $2.911 \leqslant \sqrt{s} \leqslant 3.617$ GeV. The data (open circles) are from Ref. [14]: $\sqrt{s} = 2.911$ GeV (a); 2.950 GeV (b); 2.975 GeV (c); 2.979 GeV (d); 2.981 GeV (e); 2.985 GeV (f); 2.990 GeV (g); 2.994 GeV (h); 3.005 GeV (i); 3.097 GeV (j); 3.526 GeV (k); 3.592 GeV (l); 3.617 GeV (m). The calculation is the solid, red line.

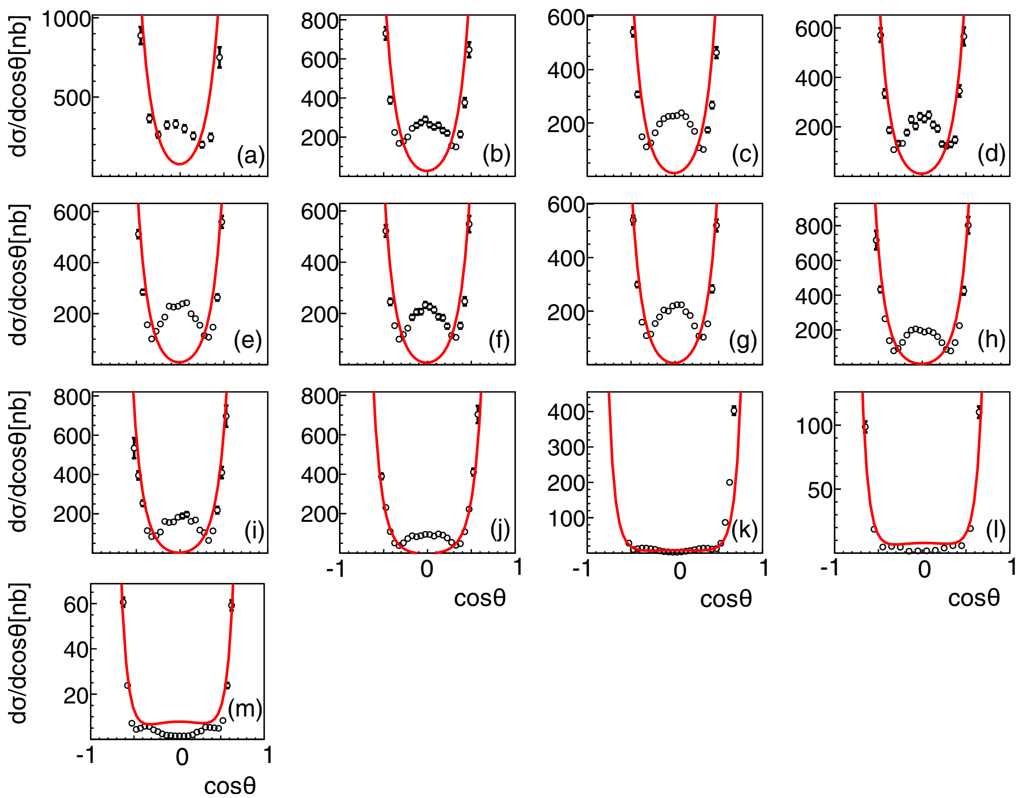

FIG. 9. Same as Fig. 8, but for the reaction $\bar{p}p \to \eta\pi^0$.

annihilation in the energy range $2.2 \leqslant \sqrt{s} \leqslant 4.4$ GeV. Note that the present work is the first attempt to describe such large set of data in the considered energy range. Previous approaches based on (relativistic) quark models that were mostly developed in connection with the LEAR experiments (see, for example, Refs. [8,21–24]) pointed out the complicated features of the annihilation and of the nonperturbative structure of hadrons. The present model, based on baryon and meson exchanges, is an effective way to take into account the quark dynamics. In this energy range, we are convinced that such an approach is convenient and has a certain predictive power as long as a reasonable number of exchanged particles and diagrams is sufficient to describe that experimental data. The main advantages is that the number of parameters can be limited and these parameters have generally a physical meaning. The logarithmic expression for s- and t (u)-dependent form factors is shown to be convenient in this nonperturbative region, where the Regge description does not apply yet and the exponential dependence does not fit to the experimental data. Note that a logarithmic expression is what reproduces best the time-like form factor of the proton. In Ref. [25] it was suggested that it is related to the time scale of the hadronization process.

Coupling constants are fixed from the properties of the known decay width. The agreement with the existing data from Ref. [14] is satisfactory for the angular dependence as well as for the energy dependence of the cross section, especially at high energy. In particular the model is able to describe very nicely the available data for $\pi^0\pi^0$ production at $\sqrt{s} = 4.274$ GeV.

Around $\cos\theta = 0$, the model follows naturally the expected behavior from quark counting rules, concerning the s dependence. However, the bump in the central region, present at low energies, is missed by the model. Possible improvement is foreseen by adding other components that, however, should vanish as the energy increases. A fine tuning is desirable, and will be more meaningful when more data will be available at PANDA, in a larger and more complete angular and energy range. The implementation to Monte Carlo simulations for predictions and optimization to the forthcoming PANDA experiment is foreseen for this aim, too.

Using SU(3) symmetry, without any change of parameters, the angular distributions are recovered for $\bar{p} + p \to \eta + \eta$ and for the asymmetric reaction $\bar{p} + p \to \pi^0 + \eta$.

ACKNOWLEDGMENTS

Thanks are due to D. Marchand and A. E. Dorokhov for useful discussions and interest in this work. Yu.B acknowledges kind hospitality at IPN Orsay, in the frame of a JINR-IN2P3 agreement and the support of the Heisenberg-Landau program (HLP-2017-11). Y.W. acknowledges support from the Chinese CSC Scholar program.

APPENDIX A: s-EXCHANGE OF NEUTRAL SCALAR MESONS: f_0 CONTRIBUTION

The matrix element is written as

$$i\mathcal{M}_{f_0} = -\frac{g_{f_0NN}\,g_{f_0\pi\pi}}{q_s^2 - m_{f_0}^2 + i\sqrt{q_s^2}\Gamma_{f_0}\big(q_s^2\big)}\bar{v}(p_1)u(p_2). \tag{A1}$$

Squaring the amplitude one finds

$$|\mathcal{M}|^2 = \frac{g_{f_0NN}^2\,g_{f_0\pi\pi}^2}{\big|q_s^2 - m_{f_0}^2 + i\sqrt{q_s^2}\Gamma_{f_0}\big(q_s^2\big)\big|^2}2(s-4M^2). \tag{A2}$$

1. $f_0\pi\pi$ coupling constant

The decay width of the f_0 meson in the system where it is at rest is given by

$$d\Gamma(f_0 \to \pi\pi) = \frac{1}{2m_{f_0}}|\mathcal{M}(f_0 \to \pi\pi)|^2 d\Phi_2, \tag{A3}$$

with the phase space

$$d\Phi_2 = \frac{\Lambda^{1/2}(m_{f_0},m_\pi,m_\pi)}{2^5\pi^2 m_{f_0}^2}d\Omega, \quad \Lambda^{1/2}(m_{f_0},m_\pi,m_\pi) = M^2\sqrt{1-\frac{4m_\pi^2}{M_p^2}}. \tag{A4}$$

Therefore

$$\Phi_2 = \frac{\Lambda^{1/2}(m_{f_0},m_\pi,m_\pi)}{2^3\pi}\sqrt{1-\frac{4m_\pi^2}{M_p^2}}. \tag{A5}$$

The matrix element for the decay $f_0 \to \pi\pi$ is (see Fig. 2)

$$\mathcal{M}(f_0 \to \pi\pi) = \frac{1}{(2\pi)^4}g_{f_0\pi\pi}. \tag{A6}$$

2. f_0 interferences

N-f_0 interference:

$$2\mathrm{Re}[\mathcal{M}_N^*\mathcal{M}_{f_0}] = 2\mathrm{Re}\,\frac{g_{f_0NN}\,g_{f_0\pi\pi}\,g_{\pi NN}^2}{\big[s - m_{f_0}^2 - i\sqrt{s}\Gamma_{f_0}(s)\big]\big(t - M_p^2\big)}\mathrm{Tr}[(\hat{p}_1 - M_p)(-\hat{q}_t + M_p)(\hat{p}_2 + M_p)]. \tag{A7}$$

Δ-f_0 interference:

$$\begin{aligned}2\mathrm{Re}[\mathcal{M}_\Delta^*\mathcal{M}_{f_0}] &= 2\mathrm{Re}\,\frac{g_{f_0NN}\,g_{f_0\pi\pi}\,g_{\Delta NN}^2}{\big[s - m_{f_0}^2 - i\sqrt{s}\Gamma_{f_0}(s)\big]\big(t - M_\Delta^2\big)}\\ &\quad\times \mathrm{Tr}[(\hat{p}_1 - M_p)(-\hat{q}_t + M_\Delta)\tilde{P}_{\alpha\beta}(\hat{p}_2 + M_p)]k_1^\alpha k_2^\beta.\end{aligned} \tag{A8}$$

APPENDIX B: s-EXCHANGE OF NEUTRAL SCALAR MESONS: f_2 CONTRIBUTION

Let us consider $f_2(1270)$ with spin 2 and positive parity that decays ∼100% into two neutral pions.

1. f_2 propagator

The f_2 propagator is

$$\frac{\chi_{\mu\nu}\chi_{\alpha\beta}}{q_s^2 - m_{f_2}^2 + i\sqrt{q_s^2}\Gamma_{f_2}\big(q_s^2\big)}, \tag{B1}$$

where the width of the f_2 is taken into account by the Breit-Wigner function and the transferred momentum is $q_s = p_1 + p_2 = k_1 + k_2$, $q_s^2 = s$.

2. Vertex $f_2 \to pp$

The Lagrangian for the decay $f_2 \to pp$ is written as

$$\mathcal{L}_{f_2\bar{p}p} = g_{f_2pp}\bar{p}\big(\gamma_\mu i\partial_\nu + \gamma_\nu i\partial_\mu + \tfrac{2}{3}\eta_{\mu\nu}i\hat{\partial}\big)pT^{\mu\nu}. \tag{B2}$$

The last term in Eq. (B2) vanishes since it is the product of an antisymmetric and a symmetric tensor.

The vertex $f_2 \to pp$ then is written as [see Fig. 1(c)]

$$(-i)g_{f_2pp}\gamma_\mu(p_1 - p_2)_\nu\chi^{\mu\nu}, \tag{B3}$$

where the symmetric tensor $\chi^{\mu\nu}$ has the following properties:

$$\chi_{\mu\nu} = \chi_{\nu\mu}, \quad \chi_{\mu\nu}g^{\mu\nu} = 0, \quad \chi_{\mu\nu}q^\nu = 0; \quad \chi_{\mu\nu}\chi_{\alpha\beta} = \tfrac{1}{2}(\eta_{\alpha\nu}\eta_{\nu\beta} + \eta_{\mu\beta}\eta_{\nu\alpha}) - \tfrac{1}{3}\eta_{\mu\nu}\eta_{\alpha\beta}, \tag{B4}$$

with $\eta_{\mu\nu} = -g_{\mu\nu} + \dfrac{q_\mu q_\nu}{q^2}$, and q is the f_2 meson four-momentum.

3. Vertex $f_{2\pi\pi}$

The amplitude for the $f_2 \to \pi\pi$ decay is

$$\mathcal{M}(f_2 \to \pi\pi) = -\frac{-1}{(2\pi)^4}(-i)g_{f_2\pi\pi}\chi^{\mu\nu}\Theta^\pi_{\mu\nu}, \tag{B5}$$

where $g_{f_2\pi\pi}$ is the constant for the decay $f_2 \to \pi\pi$ and

$$\Theta^\pi_{\mu\nu} = \tfrac{1}{2}\eta_{\mu\nu}(\partial_\alpha\pi)^2 - (\partial_\mu\pi)(\partial_\nu\pi), \tag{B6}$$

which results in

$$\begin{aligned}\mathcal{M}(f_2 \to \pi\pi) &= (-i)\frac{1}{2}g_{f_2\pi\pi}\chi^{\mu\nu}\left[2\frac{1}{2}\eta_{\mu\nu}(k_1k_2) - k_{1\mu}k_{2\nu} - k_{1\nu}k_{2\mu}\right]\\ &= \frac{i}{2}g_{f_2\pi\pi}\chi^{\mu\nu}\big[k_{1\mu}k_{2\nu} + k_{1\nu}k_{2\mu} - (k_1k_2)\eta_{\mu\nu}\big].\end{aligned} \tag{B7}$$

The matrix element for the f_2 s-channel exchange in $\bar{p}p \to \pi^0\pi^0$ is

$$\mathcal{M}_{f_2} = \frac{g_{f_2pp}g_{f_2\pi\pi}}{2}[\bar{v}(p_1)\gamma_\mu(p_2 - p_1)_\nu u(p_2)]\frac{F^{\mu\nu\alpha\beta}}{s - m^2_{f_2} + i\sqrt{s}\Gamma_{f_2}}[k_{1\alpha}k_{2\beta} + k_{1\beta}k_{2\alpha} - (k_1k_2)\eta_{\alpha\beta}],$$

$$\mathcal{M}^*_{f_2} = \frac{g_{f_2pp}g_{f_2\pi\pi}}{2}[\bar{u}(p_2)\gamma_\rho(p_2 - p_1)_\sigma v(p_1)]\frac{F^{\rho\sigma\gamma\delta}}{s - m^2_{f_2} - i\sqrt{s}\Gamma_{f_2}}[k_{1\gamma}k_{2\delta} + k_{1\delta}k_{2\gamma} - (k_1k_2)\eta_{\gamma\delta}],$$

where $F^{\mu\nu\alpha\beta} = \chi_{\mu\nu}\chi_{\alpha\beta}$. The matrix element squared is

$$\begin{aligned}|\mathcal{M}_{f_2}|^2 = {}& \frac{g^2_{f_2pp}g^2_{f_2\pi\pi}}{4}\frac{F^{\mu\nu\alpha\beta}F^{\rho\sigma\gamma\delta}}{\left|s - m^2_{f_2} + i\sqrt{s}\Gamma_{f_2}\right|^2}\mathrm{Tr}[(\hat{p}_1 - M)\gamma_\mu(p_2 - p_1)_\nu(\hat{p}_2 + M)\gamma_\rho(p_2 - p_1)_\sigma]\\ &\times[k_{1\alpha}k_{2\beta} + k_{1\beta}k_{2\alpha} - (k_1k_2)\eta_{\alpha\beta}][k_{1\gamma}k_{2\delta} + k_{1\delta}k_{2\gamma} - (k_1k_2)\eta_{\gamma\delta}].\end{aligned} \tag{B8}$$

The decay width of the f_2 meson in the system where it is at rest is given by

$$d\Gamma(f_2 \to \pi\pi) = \frac{g^2_{f_2\pi\pi}}{2m_{f_2}}|\mathcal{M}(f_2 \to \pi\pi)|^2 d\Phi_2, \tag{B9}$$

with the phase space

$$d\Phi_2 = \frac{\Lambda^{1/2}(m_{f_2},m_\pi,m_\pi)}{2^5\pi^2m^2_{f_2}}d\Omega, \quad \Lambda^{1/2}(m_{f_2},m_\pi,m_\pi) = m^2_{f_2}\sqrt{1 - \frac{4m^2_\pi}{m^2_{f_2}}}. \tag{B10}$$

Therefore

$$\Phi_2 = \frac{\Lambda^{1/2}(m_{f_2},m_\pi,m_\pi)}{2^3\pi}\sqrt{1 - \frac{4m^2_\pi}{m^2_{f_2}}}. \tag{B11}$$

The matrix element for the decay $f_2 \to \pi\pi$ is [see Fig. 2(c)]

$$|\mathcal{M}(f_2 \to \pi\pi)|^2 = \frac{1}{4}\frac{F^{\mu\nu\alpha\beta}F^{\rho\sigma\gamma\delta}}{\left|s - m_{f_2}^2 + i\sqrt{s}\Gamma_{f_2}\right|^2}[k_{1\alpha}k_{2\beta} + k_{1\beta}k_{2\alpha} - (k_1k_2)\eta_{\alpha\beta}][k_{1\gamma}k_{2\delta} + k_{1\delta}k_{2\gamma} - (k_1k_2)\eta_{\gamma\delta}], \tag{B12}$$

$$\Gamma_{f_2} = \frac{g_{f_2\pi\pi}^2}{16m_{f_2}\pi}|\mathcal{M}(f_2 \to \pi\pi)|^2\sqrt{1 - \frac{4m_\pi^2}{m_{f_2}^2}}. \tag{B13}$$

Taking the value $\Gamma = (0.1867 \pm 0.0025)$ GeV, one finds $g_{f_2\pi\pi} = (19 \pm 0.26)\ \mathrm{GeV}^{-1}$.

4. f_2 interferences

f_0-f_2 interference:

$$2\mathrm{Re}[\mathcal{M}_{f_0}^*\mathcal{M}_{f_2}] = -\mathrm{Re}\frac{g_{f_0NN}g_{f_0\pi\pi}g_{f_2NN}g_{f_2\pi\pi}}{\left[s - m_{f_0}^2 - i\sqrt{s}\Gamma_{f_0}(s)\right]\left[s - m_{f_2}^2 + i\sqrt{s}\Gamma_{f_2}(s)\right]}F^{\mu\nu\alpha\beta}[k_{1\alpha}k_{2\beta} + k_{1\beta}k_{2\alpha} - (k_1k_2)\eta_{\alpha\beta}]$$
$$\times\,\mathrm{Tr}[(\hat{p}_1 - M_p)\gamma_\mu(p_2 - p_1)_\nu(\hat{p}_2 + M_p)]. \tag{B14}$$

N-f_2 interference:

$$2\mathrm{Re}[\mathcal{M}_{f_2}\mathcal{M}_N^*] = \mathrm{Re}\frac{g_{f_2NN}g_{f_2\pi\pi}g_{\pi NN}^2}{\left[s - m_{f_2}^2 + i\sqrt{s}\Gamma_{f_2}(s)\right]\left(t - M_p^2\right)}F^{\mu\nu\alpha\beta}[k_{1\alpha}k_{2\beta} + k_{1\beta}k_{2\alpha} - (k_1k_2)\eta_{\alpha\beta}]$$
$$\times\,\mathrm{Tr}[(\hat{p}_1 - M_p)\gamma_\mu(p_2 - p_1)_\nu(\hat{p}_2 + M_p)(-\hat{q}_t + M_p)]. \tag{B15}$$

Δ-f_2 interference:

$$2\mathrm{Re}[\mathcal{M}_\Delta^*\mathcal{M}_{f_2}] = -\mathrm{Re}\frac{g_{f_2NN}g_{f_2\pi\pi}g_{N\Delta N\pi}^2}{\left[s - m_{f_2}^2 + i\sqrt{s}\Gamma_{f_2}(s)\right]\left(t - M_\Delta^2\right)}F^{\mu\nu\alpha\beta}[k_{1\alpha}k_{2\beta} + k_{1\beta}k_{2\alpha} - (k_1k_2)\eta_{\alpha\beta}]$$
$$\times\,\mathrm{Tr}[(\hat{p}_1 - M_p)\gamma_\mu(p_2 - p_1)_\nu(\hat{p}_2 + M_p)P_{\rho\sigma}(q)(\hat{q}_t + M_\Delta)]k_1^\sigma k_2^\delta. \tag{B16}$$

[1] Y. Wang, Y. M. Bystritskiy, and E. Tomasi-Gustafsson, Phys. Rev. C **95**, 045202 (2017).
[2] M. F. M. Lutz *et al.* (PANDA Collaboration), arXiv:0903.3905 [hep-ex].
[3] C. B. Dover, T. Gutsche, M. Maruyama, and A. Faessler, Prog. Part. Nucl. Phys. **29**, 87 (1992).
[4] E. Klempt, C. Batty, and J.-M. Richard, Phys. Rep. **413**, 197 (2005).
[5] B. Loiseau, Nucl. Phys. A **543**, 33C (1992).
[6] B. El-Bennich, M. Lacombe, B. Loiseau, and S. Wycech, Phys. Rev. C **79**, 054001 (2009).
[7] V. F. Dmitriev, A. I. Milstein, and S. G. Salnikov, Phys. Lett. B **690**, 427 (2010).
[8] G. Bathas and W. M. Kloet, Phys. Lett. B **301**, 155 (1993).
[9] B. Moussallam, Nucl. Phys. A **429**, 429 (1984).
[10] V. A. Matveev, R. M. Muradyan, and A. N. Tavkhelidze, Teor. Mat. Fiz. **15**, 332 (1973).
[11] S. J. Brodsky and G. R. Farrar, Phys. Rev. Lett. **31**, 1153 (1973).
[12] K. Olive *et al.* (Particle Data Group), Chin. Phys. C **38**, 090001 (2014).
[13] V. Baru, J. Haidenbauer, C. Hanhart, A. E. Kudryavtsev, and U.-G. Meissner, Eur. Phys. J. A **23**, 523 (2005).
[14] T. Armstrong *et al.* (Fermilab E760 Collaboration), Phys. Rev. D **56**, 2509 (1997).
[15] R. Machleidt, Phys. Rev. C **63**, 024001 (2001).
[16] V. L. Chernyak, A. R. Zhitnitsky, and V. G. Serbo, Pisma Zh. Eksp. Teor. Fiz. **26**, 760 (1977) [JETP Lett. **26**, 594 (1977)].
[17] G. P. Lepage and S. J. Brodsky, Phys. Rev. Lett. **43**, 545 (1979).
[18] M. Ablikim *et al.* (BESIII Collaboration), Phys. Lett. B **735**, 101 (2014).
[19] B. Aubert (BABAR Collaboration), Phys. Rev. D **73**, 012005 (2006).
[20] J. P. Singh, F. X. Lee, and L. Wang, Int. J. Mod. Phys. A **26**, 947 (2011).
[21] A. Muhm, T. Gutsche, R. Thierauf, Y. Yan, and A. Faessler, Nucl. Phys. A **598**, 285 (1996).
[22] B. El-Bennich and W. M. Kloet, Phys. Rev. C **70**, 034001 (2004).
[23] B. El-Bennich and W. M. Kloet, Phys. Rev. C **70**, 034002 (2004).
[24] B. El-Bennich, Phys. Rev. C **72**, 067001 (2005).
[25] A. Bianconi and E. Tomasi-Gustafsson, Phys. Rev. C **95**, 015204 (2017).